Dyes and Pigments 97 (2013) 475–480

Contents lists available at SciVerse ScienceDirect

Dyes and Pigments

journal homepage: www.elsevier.com/locate/dyepig

Short communication

A benzimidazole-based ratiometric fluorescent sensor for Cr^{3+} and Fe^{3+} in aqueous solution

Meng Wang, Jungang Wang, Weijian Xue, Anxin Wu*

Key Laboratory of Pesticide & Chemical Biology, Ministry of Education, Central China Normal University, 152 Luoyu Road, Wuhan 430079, PR China

ARTICLE INFO

Article history:
Received 24 November 2012
Received in revised form
2 February 2013
Accepted 5 February 2013
Available online 16 February 2013

Keywords:
Fluorescent sensor
Benzimidazole
Ratiometric
Cr^{3+}
Fe^{3+}
Aqueous solution

ABSTRACT

A novel ratiometric fluorescent sensor bearing two benzimidazole groups has been synthesized. The sensor showed a ratiometric fluorescence response with an enhancement of the ratios of emission intensities at 443 and 378 nm from 0.17 to 3.21 for Cr^{3+}. The ratios of emission intensities at 443 and 380 nm were enhanced from 0.40 to 2.09 for Fe^{3+}. Fe^{3+} revealed significant adsorption in the UV–vis region, which can be used to discriminate Cr^{3+} and Fe^{3+}. Detection limits of the method for Cr^{3+} and Fe^{3+} were 25 μM and 2 μM, respectively. In addition, the sensor showed good selectivity to Cr^{3+} and Fe^{3+} over other metal ions.

1. Introduction

Trivalent chromium (Cr^{3+}) and iron (Fe^{3+}) are essential nutrients for humans, playing a key role in many biochemical processes at a cellular level [1,2]. Cr^{3+} also improves insulin sensitivity, while also acting as a glucose tolerance factor through the metabolism of carbohydrates, fats, and proteins [3]. The deficiency of chromium can cause disturbances in glucose levels and lipid metabolism; on the other hand, exposure to high levels of Cr^{3+} can negatively affect cellular structures [4]. Fe^{3+} is indispensable for most organisms and both its deficiency and overload can induce various disorders such as tightly regulated iron trafficking, storage, and balance in an organism [5,6]. Nevertheless, Cr^{3+} and Fe^{3+} are well-known as fluorescence quenchers due to their paramagnetic nature [7–9] and sensors with a fluorescence enhancement signal when interacting with guests are much more efficient. In recent years, a number of fluorescent receptors for Fe^{3+} have been reported [7,8,10–13]; yet few sensors for Cr^{3+} have been described in the literature [14,15].

However, whether fluorescent sensing systems for metal ions function by fluorescence enhancement or quenching, as the change in fluorescence intensity is the only detection signal; other factors such as instrumental efficiency and environmental conditions are known to interfere with signal output [16]. Ratiometric fluorescent sensors allow for the measurement of emission intensities at two different wavelengths. Additionally, most of the foregoing sensors have revealed the dual emission system can eliminate most or all ambiguities in the detection through the self-calibration of two emission bands. Thus, the ratiometric fluorescent sensor has become one of the most promising sensing strategies for accurate detection [17]. In spite of this, both Fe^{3+} and Cr^{3+} ratiometric fluorescent sensors remain extremely scarce [18–20].

In addition, most of these sensors have revealed that the fluorescence intensity decreases sharply with an increase in water content; thus demonstrating their inability to coexist with large amounts of water [15,21,22]. Here, we report a new ratiometric fluorescent sensor for Fe^{3+} and Cr^{3+} based on a derivative of benzimidazole, which subsequently demonstrates a blue-shift and fluorescence-enhanced response toward Fe^{3+} and Cr^{3+} in aqueous solution DMSO/H_2O (1:99, v/v).

2. Experiment

2.1. Reagents

All starting materials and catalysts were obtained commercially and used without further purification. Most of the solvents were distilled under N_2 over the appropriate drying reagents (sodium or

* Corresponding author. Tel./fax: +86 27 6786 7773.
E-mail address: chwuax@mail.ccnu.edu.cn (A. Wu).

0143-7208/$ – see front matter © 2013 Elsevier Ltd. All rights reserved.
http://dx.doi.org/10.1016/j.dyepig.2013.02.005

calcium hydride). Deionized water was used throughout the experiments. Column chromatography: silica gel 200–300 mesh.

2.2. Apparatus

Absorption spectra were taken at room temperature using a UV-2501 PC spectrophotometer (SHIMADZU CORPORATION) with a variable wavelength between 200 and 900 nm and with the use of a glass cuvette with a 0.5 cm optical path. Fluorescence spectra measurements were performed on a Cary Eclipse spectrofluorometer. Slits were set to provide widths of 5 nm for the emission monochromators in all cases. NMR spectra were measured on a Varian Mercury 400 spectrometer operating at frequencies of 400 MHz for ^{1}H and 100 MHz for ^{13}C, while the Varian NMR System 600 MHz spectrometer operated at frequencies of 600 MHz for ^{1}H and 150 MHz for ^{13}C relative to tetramethylsilane as an internal standard. HRMS were obtained on an FT-ICR MS equipped with an electrospray source. IR spectra were recorded on a Tensor 27 infrared spectrometer and KBr pellets with absorption were reported in cm^{-1}. The X-ray crystal structure determination of **1a** was obtained on a Bruker SMART APEX CCD system. Melting points were determined using XT-4 apparatus and not corrected.

2.3. Synthesis of compounds *1*

The synthetic route to access the compounds is shown in Scheme 1. 1,4-Dibromo-2,3-bis(bromomethyl)benzene was prepared according to the procedures set out in the literature [23]. Compound **2** was prepared by a modification of the procedure outlined by Murray [24]. 1,4-Dibromo-2,3-bis(bromomethyl)benzene (**3**) was added to a stirred solution of benzimidazole (benzotriazole, 5,6-dimethyl-1*H*-benzo[*d*]imidazole, 2-chloro-1*H*-benzo[*d*]imidazole) and powdered NaOH in DMF and H_2O. The mixture was stirred at 60 °C for two days to give **2** in 50–92%. To a solution of bis(triphenylphosphine) palladium(II) dichloride, copper(I) iodide and compounds **2** in DMF under argon was added 4-phenylacetylene and Et_3N. After heating under reflux for 12 h, **1** was obtained at a yield of 74–80% (Scheme 2) [25–27].

2.3.1. 1,1′-((3,6-Bis(phenylethynyl)-1,2-phenylene)Bis(methylene)) Bis(1H-benzo[d]imidazole) (*1a*)

Yellow solid; yield: 0.215 g; 76%; M.p.: 114–117 °C; IR spectrum (KBr cm^{-1}): 3052, 2208, 1665, 1612, 1492, 1457, 1390, 1327, 1282, 1227, 1002, 737, 691, 536; ^{1}H NMR (600 MHz, $CDCl_3$): δ (ppm) 7.83 (d, J = 6.0 Hz, 2H), 7.79 (s, 2H), 7.64 (s, 2H), 7.327.29 (m, 8H), 7.26–7.24 (m, 9H), 5.50 (s, 4H); ^{13}C NMR (100 MHz, $CDCl_3$): δ (ppm) 143.71, 141.84, 135.48, 133.83, 133.54, 131.58, 129.17, 128.37, 126.32, 123.37, 122.63, 121.56, 120.57, 121.07, 109.62, 97.36, 85.78, 44.45 cm^{-1}; HRMS (ESI): m/z [M + H]$^+$ calcd for $C_{38}H_{27}N_4$: 539.22350; found: 539.22302.

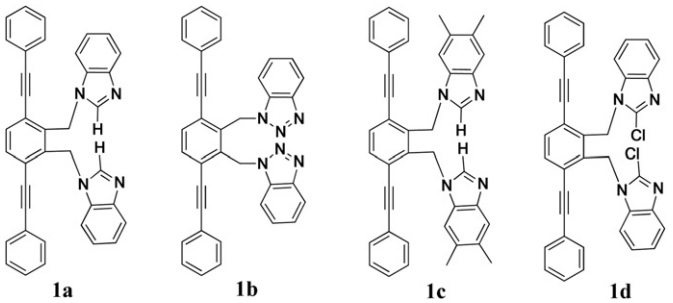

Scheme 2. Structures of the target compounds **1a**–**1d**.

2.3.2. 1,1′-((3,6-Bis(phenylethynyl)-1,2-phenylene)Bis(methylene)) Bis(5,6-dimethyl-1H-benzo[d]imidazole) (*1b*)

White solid; yield: 0.129 g; 80%; M.p.: 158–162 °C; IR spectrum (KBr cm^{-1}): 2924, 2853, 2204, 1591, 1491, 1444, 1090, 996, 831, 758, 690; ^{1}H NMR (400 MHz, $CDCl_3$): δ (ppm) 8.04 (dd, J = 4.0, 4.0 Hz, 2H), 7.75 (dd, J = 4.0, 4.0 Hz, 2H), 7.64 (s, 2H), 7.37–7.31 (m, 14H), 6.41 (s, 4H); ^{13}C NMR (100 MHz, $CDCl_3$): δ (ppm) 145.71, 136.25, 133.22, 131.50, 128.38, 127.44, 125.76, 123.89, 121.92, 119.81, 110.11, 96.98, 86.83, 47.87 cm^{-1}; HRMS (ESI): m/z [M + H]$^+$ calcd for $C_{36}H_{25}N_6$: 541.2136; found: 541.2135.

2.3.3. 1,1′-((3,6-Bis(phenylethynyl)-1,2-phenylene)Bis(methylene)) Bis(2-chloro-1H-benzo[d]imidazole) (*1c*)

Yellow solid; yield: 0.139 g; 78%; M.p. > 300 °C; IR spectrum (KBr cm^{-1}): 2923, 2362, 2206, 1591, 1494, 1218, 836, 754, 687, 430; ^{1}H NMR (600 MHz, $CDCl_3$): δ (ppm) 7.77 (s, 2H), 7.56 (s, 4H), 7.26 (m, 10H), 7.03 (s, 2H), 5.43 (s, 4H), 2.37 (s, 6H), 2.29 (s, 6H); ^{13}C NMR (150 MHz, $CDCl_3$): δ (ppm) 140.84, 135.74, 133.43, 132.65, 131.60, 129.10, 128.34, 126.29, 121.69, 120.18, 109.82, 97.09, 85.91, 44.36, 20.56, 20.24 cm^{-1}; HRMS (ESI): m/z [M + H]$^+$ calcd for $C_{42}H_{35}N_4$: 595.28637; found: 595.28562.

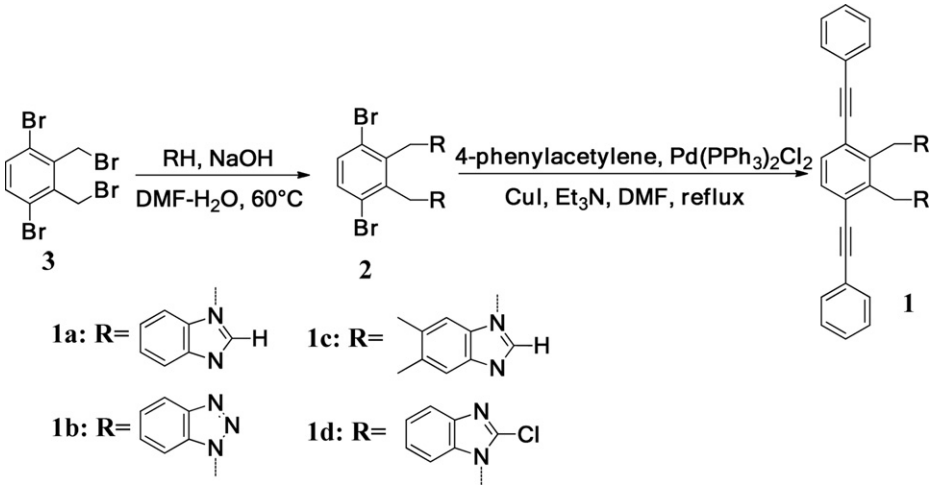

Scheme 1. Synthesis of compound **1**.

*2.3.4. 1,1′-((3,6-Bis(phenylethynyl)-1,2-phenylene)Bis(methylene)) Bis(1H-benzo[d] [1-3]triazole) (**1d**)*

Yellow solid; yield: 0.134 g; 74%; M.p.: 218–222 °C; IR spectrum (KBr cm^{-1}): 3059, 2203, 1612, 1476, 1338, 1265, 836, 734, 689, 526. ^1H NMR (400 MHz, $CDCl_3$): δ (ppm) 7.68–7.64 (m, 4H), 7.30–7.25 (m, 10H), 7.19 (t, $J = 8.0$ Hz, 2H), 7.04 (t, $J = 8.0$ Hz, 2H), 6.80 (d, $J = 8.0$ Hz, 2H), 5.67 (s, 4H); ^{13}C NMR (100 MHz, $CDCl_3$): δ (ppm) 141.69, 140.76, 135.07, 134.94, 133.86, 131.55, 129.09, 128.34, 125.58, 123.49, 122.80, 121.75, 119.64, 109.99, 98.13, 85.96, 45.49 cm^{-1}. HRMS (ESI): *m/z* $[M + H]^+$ calcd for $C_{38}H_{25}Cl_2N_4$: 607.14524; found: 607.14508.

*2.4. X-ray diffraction analysis of compound **1a***

A crystal of **1a** was grown by the slow evaporation of solutions of the compound in $CHCl_3/CH_3OH$ (8:2, v/v) and found to be suitable for X-ray crystal structure analysis. Details of the crystal data have been deposited with Cambridge Crystallographic Data Centre and are available in Supplementary Publication No. CCDC 900488.

2.5. Measurement procedures

Compound **1a**–**d** were weighed accurately, transferred to a 10 mL volumetric flask and dissolved and made up to 10 mL with DMSO. Then 1 mL of the DMSO solution was transferred into 100 mL volumetric flask and made up to the volume with deionized water to obtain the stock solutions of **1a**–**d** (10 μM) in DMSO/H_2O (1:99, v/v). The stock solutions of cations and anions were prepared in DMSO/H_2O (1:99, v/v) with a concentration of 3.0×10^{-3} M for fluorescence spectral analysis and UV–vis adsorption spectrum. Each time a 3 mL solution of **1** was filled to a quartz cell of 1 cm optical path length, the concentrations of cations and anions were increased by the addition of different equivalents using a micro-syringe. All the experiments used an excitation wavelength of 320 nm and room temperature.

3. Results and discussion

*3.1. Structural characteristics of **1a***

A single crystal of **1a**·CH_3OH suitable for crystallography was obtained from the slow evaporation of a concentrated $CHCl_3/CH_3OH$ (8:2, v/v) solution of **1a** at ambient temperature. The structure of **1a** is depicted in Fig. 1. Two independent molecules in the unit cell were visible. The two benzimidazole rings of one molecule formed a dihedral angle of 22°. The distance between C23B and C24B of the benzimidazole group was 3.184 Å. The CH_3OH molecule played a key role in stabilizing the crystal structure by providing an electron donor (oxygen atom).

3.2. Spectral characteristics

As shown in Fig. 2, compound **1a** exhibited a strong absorption band centered at 328 and 230 nm in DMSO/H_2O (1:99, v/v); the compound **1b**–**1d** demonstrated a similar characteristic absorption peak (Figs. S1–S3). The high-energy peak at around 328 and 230 nm was due to the $\pi \rightarrow \pi^*$ electronic transition. Receptor **1a** displayed a well-defined maximum at 443 nm in the fluorescence spectrum and recorded a concentration of 10 μM in DMSO/H_2O (1:99, v/v) when excited at 320 nm. A similar peak was found in **1b**–**1d**, which held the same luminescent fragments (Figs. S4–S6).

3.3. Selectivity

The cation binding affinity of sensor **1** toward different alkali, alkaline earth, and transition metal ions was investigated with

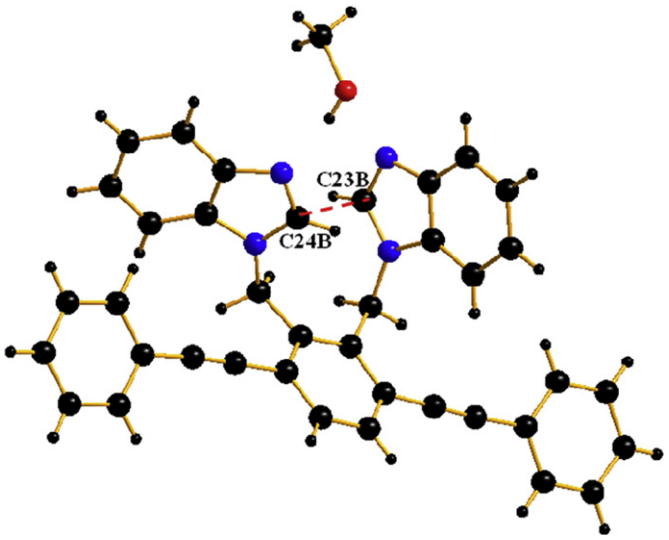

Fig. 1. Crystal structure of **1a**·CH_3OH.

fluorescence and UV–vis absorption spectroscopy. The selectivity of **1a** for Cr^{3+} and Fe^{3+} over other common metal ions at a biological concentration level was examined in DMSO/H_2O (1:99, v/v, 10 μM). Fig. 3 indicates that the addition of K^+, Ba^{2+}, Sr^{2+}, Mg^{2+}, Zn^{2+}, Co^{2+}, Cd^{2+}, Pb^{2+}, Hg^{2+}, Mn^{2+}, Ni^{2+}, and La^{3+} caused virtually no change to the fluorescence spectrum of receptor **1a**. The addition of Cu^{2+} and Ag^+ caused a minor decrease in the emission intensity, which can be attributed to the fact that these transition and heavy metal ions have an intrinsic quenching nature [28–31]. In contrast, the addition of Cr^{3+}/Fe^{3+} to the solution of receptor **1a** resulted in a drastic fluorescence emission change. A steady decrease in emission intensity at 443 nm was observed, along with a concomitant increase in the intensity of the new fluorescence band at 378/380 nm (up to 6.0/4.9-fold enhancement when compared to the fluorescence intensity of free sensor **1a** at 378 nm, see Fig. 3B). The selectivity of Cr^{3+}/Fe^{3+} was calculated via a selectivity coefficient ($K_{Cr^{3+}/Fe^{3+}} = S_{Cr^{3+}/Fe^{3+}}/S_0$), where $S_{Cr^{3+}/Fe^{3+}}$ was the response to Cr^{3+}/Fe^{3+} and S_0 was the response to other cations [32]. The selectivity coefficients of Cr^{3+}/Fe^{3+} measured

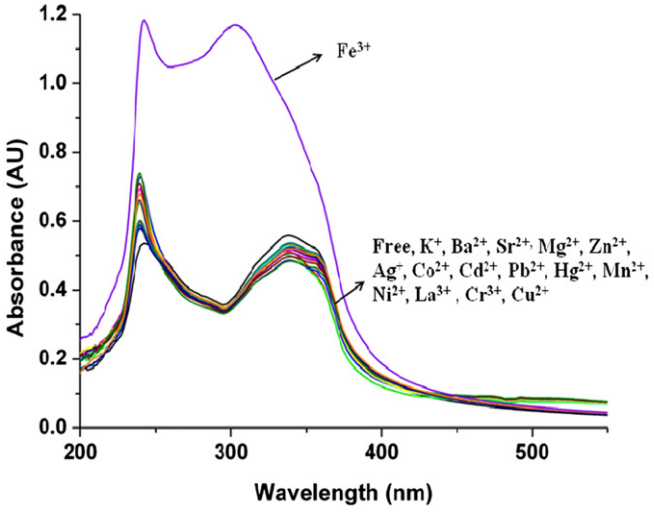

Fig. 2. UV–vis adsorption spectrum of **1a** (10 μM) on addition of 50 equiv of different metal ions in DMSO/H_2O (1:99, v/v).

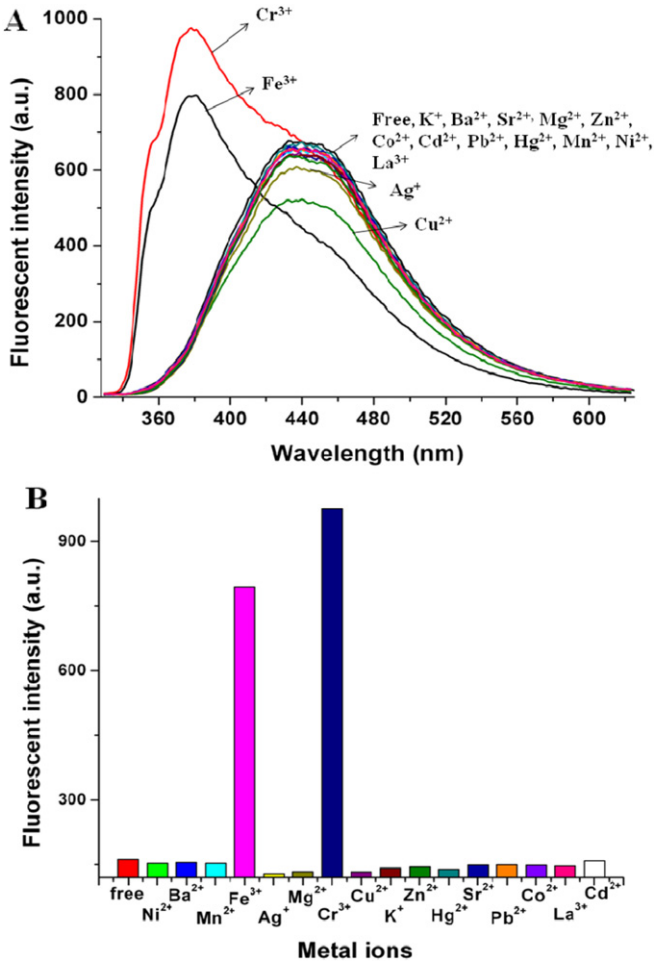

Fig. 3. (A) Changes in the fluorescence spectrum of **1a** (10 μM) upon addition of metal salts in DMSO/H_2O (1:99, v/v) with excitation at 320 nm (30 equiv). (B) A bar diagram showing fluorescence intensity in the presence of different metals at 378 nm.

against other tested cations are listed in Tables S1 and S2. The coefficients clearly indicated that sensor **1a** had better selectivity for Cr^{3+} and Fe^{3+} than other cations. The experiments of the counter ion effect on the selective properties of Cr^{3+}/Fe^{3+} were also measured (Fig. 4). The addition of $CrCl_3$, $FeCl_3$, and $Fe(NO_3)_3$ all had a similar influence as that of $Cr(NO_3)_3$ and $Fe(ClO_4)_3$, which implied that a different counter ion did not affect the binding of Cr^{3+}/Fe^{3+} with receptor **1a**.

The absorption spectra of compound **1a** (10 μM) in DMSO/H_2O (1:99, v/v) were also investigated (Fig. 2). The addition of 50 equiv of $Fe(ClO_4)_3$ led to the great increase of the original absorbance. Other metal ions including Cr^{3+} caused no change to the absorption intensity, which can be used to discriminate between Cr^{3+} and Fe^{3+}. Such adsorption change may be ascribed to the paramagnetic effect of Fe^{3+} [33]. Fig. 4 showed that Fe^{3+} has a substantial absorbance in the UV and near visible range. Fig. 5 showed the absorbance spectrum of receptor **1a** in the presence and absence of $Fe(ClO_4)_3$ in DMSO/H_2O (1:99, v/v). We found that the absorbance intensity of receptor **1a** in the presence of $Fe(ClO_4)_3$ was equal to the absorbance intensity of receptor **1a** and $Fe(ClO_4)_3$ (Fig. 6).

3.4. Ratiometric response to Cr^{3+} and Fe^{3+}

In order to evaluate sensor **1a** as a fluorescent sensor for Cr^{3+} and Fe^{3+}, titrations were performed with successive additions of

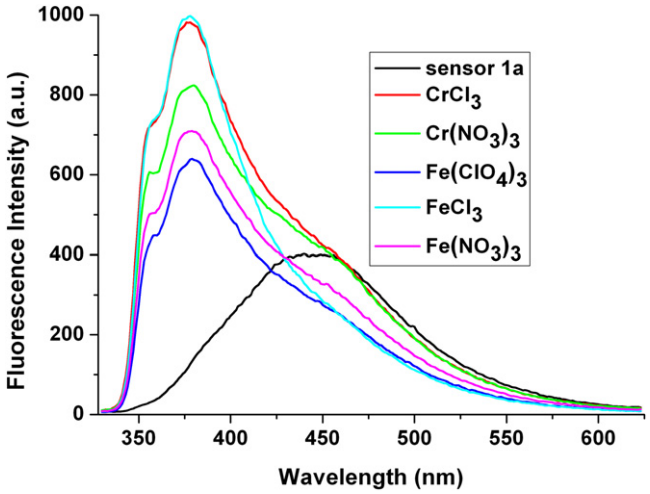

Fig. 4. Fluorescence spectra of sensor **1a** (10 μM) in DMSO/H_2O (1:99, v/v) upon addition of different Cr^{3+}/Fe^{3+} salts with excitation at 320 nm.

Cr^{3+} and Fe^{3+} to a solution of **1** in DMSO/H_2O (1:99, v/v). This led to the same type of profile as observed in Fig. 3A (Figs. 7 and 8). The fluorescence peak quenching in the fluorescence intensity of **1a** was seen at 443 nm, while the enhancement was seen at 378/380 nm. Such changes at two wavelengths offered an interesting opportunity for the ratiometric fluorescence determination of analytes. A linear relationship was obtained within a concentration range of 0–310 μM for Cr^{3+} and 0–240 μM for Fe^{3+} (inset of Figs. 7 and 8, respectively), and the linear regression parameters were 0.99372 and 0.95669 respectivly. The ratios of emission intensities at 378 and 443 nm (I_{378}/I_{443}) enhanced from 0.17 to 3.21 for Cr^{3+}, while the ratios of emission intensities at 380 and 443 nm varied from 0.40 to 2.09 for Fe^{3+}. The association constants (K_a) of receptor **1a** for Cr^{3+} and Fe^{3+} were calculated on the basis of a Hill plot (Figs. S7 and S8) [34,35]. It was found to be 1.75×10^3 M^{-1} and 8.51×10^4 M^{-1} (error limits $\leq$ 8%), respectively. The detection limit emerged to be 25 μM for Cr^{3+} and 2 μM for Fe^{3+} from 10 blank solutions based on the definition by IUPAC ($C_{DL} = 3\ S_b/m$) [36]. In both cases, the stoichiometries of the complex were determined to be 1:1 by Job's plot (Figs. S9 and S10).

3.5. Quantum yields

The fluorescent quantum yield of the compound **1a** before and after the addition of Cr^{3+} and Fe^{3+} ions was measured by

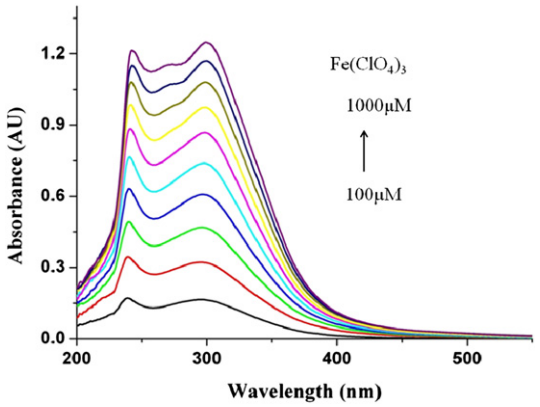

Fig. 5. The absorption spectra of $Fe(ClO_4)_3$ in DMSO/H_2O (1:99, v/v) with increasing concentrations.

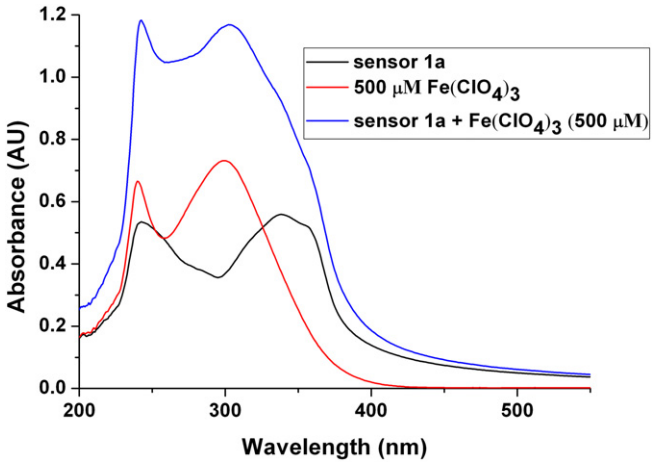

Fig. 6. The absorption spectra of $Fe(ClO_4)_3$ (500 μM), sensor **1a** (10 μM), sensor **1a** + $Fe(ClO_4)_3$ (500 μM) in DMSO/H_2O (1:99, v/v).

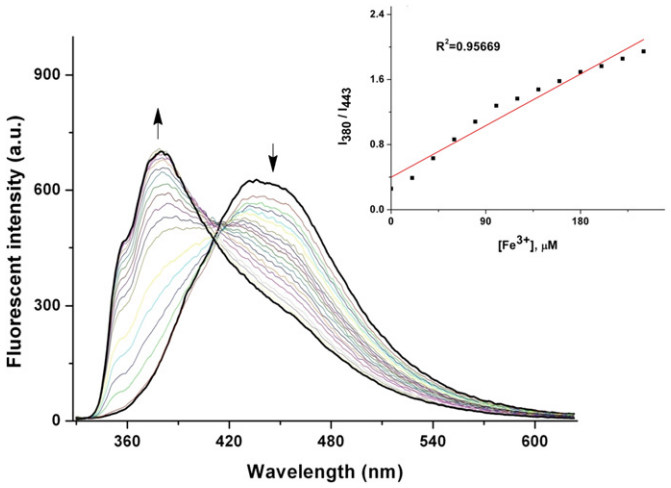

Fig. 8. Fluorescence spectra changes (λ_{ex} = 320 nm) of receptor **1a** (10 μM) upon addition of Fe^{3+} (0–30 equiv) in DMSO/H_2O (1:99, v/v).

comparison with quinine sulfate as the standard compound in sulfuric acid according to the following equation [37,38]:

$$\Phi_u = \frac{\Phi_s \times A_s \times F_u \times n^2}{A_u \times F_s \times n_0^2}$$

where Φ_u and Φ_s are quantum yield for the sample and reference, F_u and F_s are the integrated area under the corrected fluorescence spectra for the sample and reference, A_u and A_s are the absorbance for the sample and reference, n and n_0 are the refractive indexes of the solvents used for samples and reference. The quantum yield of compound **1a** was 0.92. After the addition of Cr^{3+} ions, the quantum yield increased to 1.43. While the quantum yield decreased to 0.59 after the addition of Fe^{3+} ions because the intrinsic quenching phenomenon was so evident.

3.6. Possible mechanism

Compound **1b** and **1d** were synthesized to have a comparison with **1a**. In **1b**, the C–H group was replaced by N atom. **1b** was found to be non-selective for any metal ions except Fe^{3+}, where intrinsic fluorescence quenching was demonstrated (Figs. S5 and S6). While in **1d**, the hydrogen atom was substituted by chlorine atom. Interestingly, compound **1d** also showed no selection for any metal ions except Fe^{3+}. We doubt that the C–H group of the benzimidazole was meant to complex with Cr^{3+}/Fe^{3+}. In order to confirm our hypothesis further, we synthesized **1c** retaining the C–H site to evaluate the metal ion recognition behavior. Compound **1c** had the same effect with sensor **1a** when binding with Cr^{3+}/Fe^{3+}, along with a sharp decrease in the fluorescence intensity as compared with **1a** especially for Fe^{3+} (Figs. S4); a feature which was due to the intrinsic fluorescence quenching of Fe^{3+}. The blue-shift in the fluorescence of **1a** and **1c** can be attributed to an intramolecular charge transfer (ICT), while the enhancement of fluorescence intensity upon Cr^{3+}/Fe^{3+} complexation was most likely due to photoinduced electron transfer (PET) processes [15,18]. According to the above analysis, we considered that the C–H group of the benzimidazole may have played a key role in binding with Cr^{3+} and Fe^{3+}. It was already known that Cr^{3+}/Fe^{3+} both have a strong binding affinity with receptors possessing sp^2 nitrogen of imidazole [39–41]. The Cr^{3+}/Fe^{3+} ions were assumed to have a hexahedral geometry in the complex, in which receptor **1a** acted as a tetradentate ligand while the other two coordination sites were occupied by anions.

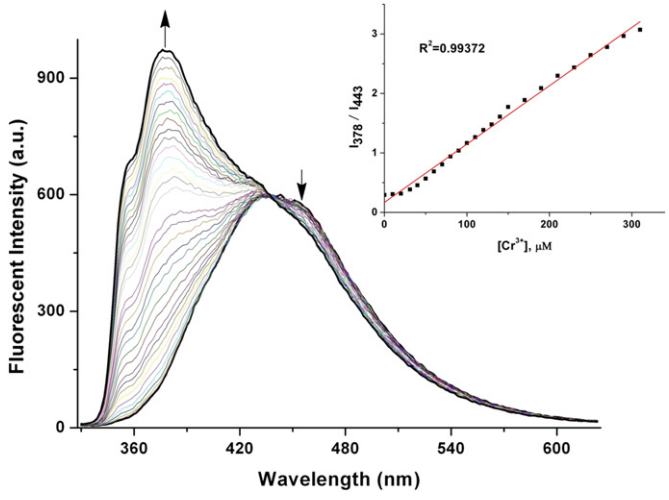

Fig. 7. Changes in the fluorescence intensity of spectrum of sensor **1a** (10 μM) with increasing concentrations of Cr^{3+} (0–35 equiv) in DMSO/H_2O (1:99, v/v).

4. Conclusion

In conclusion, we have synthesized a novel ratiometric fluorescent sensor capable of recognizing and estimating the concentrations of Cr^{3+} and Fe^{3+} in aqueous solution. It is worthy to note that examples of ratiometric fluorescent sensors for Cr^{3+} and Fe^{3+} have been very sparse. Fe^{3+} ions showed significant absorption in the UV/Visible region and thus can be discriminated from Cr^{3+} through this method. Significantly, treatment with Cr^{3+} and Fe^{3+} caused the sensor to display a ratiometric fluorescent response with a blue-shift and fluorescent enhancement. The sensor also exhibited selectivity for Cr^{3+} and Fe^{3+} above other metal ions.

Acknowledgments

We thank the National Natural Science Foundation of China (Grant 21272085). We are also grateful to Xianggao Meng for his help with X-ray diffraction analysis.

Appendix A. Supplementary data

Supplementary data related to this article can be found at http://dx.doi.org/10.1016/j.dyepig.2013.02.005.

References

[1] Aisen P, Marianne WR, Leibold EA. Iron metabolism. Curr Opin Chem Biol 1999;3:200–6.
[2] Eisenstein RS. Iron regulatory proteins and the molecular control of mammalian iron metabolism. Annu Rev Nutr 2000;20:627–62.
[3] Anderson R, Chromium RA. Trace elements in human and animal nutrition. New York: Academic Press; 1987.
[4] Zayed M, Norman T. Chromium in the environment: factors affecting biological remediation. Plant Soil 2003;249:139–56.
[5] Gupta V, Jain AK, Shiva A. An iron(III) ion-selective sensor based on a μ-bis(-tridentate) ligand. Talanta 2007;71:1964–9.
[6] Li ZX, Zhang LF, Li XY. A fluorescent color/intensity changed chemosensor for Fe^{3+} by photo-induced electron transfer (PET) inhibition of fluoranthene derivative. Dyes Pigment 2012;94:60–5.
[7] Xiang Y, Tong AJ. A new rhodamine-based chemosensor exhibiting selective FeIII-amplified fluorescence. Org Lett 2006;8:1549–53.
[8] Bricks JL, Kovalchuk A, Trieflinger C. On the development of sensor molecules that display FeIII-amplified fluorescence. J Am Chem Soc 2005;127:13522–9.
[9] Mao J, Wang L, Dou W, Tang XL. Tuning the selectivity of two chemosensors to Fe(III) and Cr(III). Org Lett 2007;9:4567–70.
[10] Li L, She NF, Fei Z. Novel fluorescent molecular clips: selective recognition towards Fe^{3+} in aqueous solution. J Fluoresc 2011;21:1103–9.
[11] Lee DY, Singh N, Jang DO. Fine tuning of a solvatochromic fluorophore for selective determination of Fe^{3+}: a new type of benzimidazole-based anthracene-coupled receptor. Tetrahedron Lett 2011;52:1368–71.
[12] Weerasinghe AJ, Schmiesing C, Varaganti S. Single- and multiphoton turn-on fluorescent Fe^{3+} sensors based on bis(rhodamine). J Phys Chem B 2010;114:9413–9.
[13] Weerasinghe AJ, Abebe FA, Sinn E. Rhodamine based turn-ON dual sensor for Fe^{3+} and Cu^{2+}. Tetrahedron Lett 2011;52:5648–51.
[14] Weerasinghe AJ, Schmiesing C, Sinn E. Highly sensitive and selective reversible sensor for the detection of Cr^{3+}. Tetrahedron Lett 2009;50:6407–10.
[15] Zhou ZG, Yu MX, Yang HY. FRET-based sensor for imaging chromium(III) in living cells. Chem Commun 2008;44:3387–9.
[16] Lee SH, Kumar J, Tripathy SK. Thin film optical sensors employing polyelectrolyte assembly. Langmuir 2000;16:10482–9.
[17] Chen J, Zeng F, Wu S, Su J. Photoreversible fluorescent modulation of nanoparticles via one-step miniemulsion polymerization. Small 2009;5:970–8.
[18] Lin WY, Long LL, Yuan L, Cao ZC. A novel ratiometric fluorescent Fe^{3+} sensor based on a phenanthroimidazole chromophore. Anal Chim Acta 2009;634:262–6.
[19] Saluja P, Sharma H, Kaur N. Benzimidazole-based imine-linked chemosensor: chromogenic sensor for Mg^{2+} and fluorescent sensor for Cr^{3+}. Tetrahedron 2012;68:2289–93.
[20] Wang DP, Shiraishi Y, Hirai T. A distyryl BODIPY derivative as a fluorescent probe for selective detection of chromium(III). Tetrahedron Lett 2010;51:2545–9.
[21] Andrea BB, Ana MC, Gil S. A new selective fluorogenic probe for trivalent cations. Chem Commun 2012;48:3000–2.
[22] Subarna G, Sisir L, Arnab B. Thiophene anchored coumarin derivative as a turn-on fluorescent probe for Cr^{3+}: cell imaging and speciation studies. Talanta 2012;91:18–25.
[23] Lai YH, Yap AH. Synthesis and rigid conformers of 14,15-dimethyl-2,11-dithia [3.3](1,3)(l,4)cyclophane and 12,13-dimethyl[2.2](1,3)(1,4)cyclophane. J Chem Soc Perkin Trans 1993;49:1373–7.
[24] Murray VB, Mark JB, David HB. Azolium-linked cyclophanes: a comprehensive examination of conformations by 1H NMR spectroscopy and structural studies. J Org Chem 2004;69:7640–52.
[25] Petricci E, Radi M, Corelli F, Botta M. Microwave-enhanced sonogashira coupling reaction of substituted pyrimidinones and pyrimidine nucleosides. Tetrahedron Lett 2003;44:9181–4.
[26] Gay RM, Flávia M, Schneider CC, Barancelli DA. $FeCl_3$-diorganyl dichalcogenides promoted cyclization of 2-alkynylanisoles to 3-chalcogen benzo[*b*]furans. J Org Chem 2010;75:5701–6.
[27] Zeni G, Larock RC. Synthesis of heterocycles via palladium π-olefin and π-alkyne chemistry. Chem Rev 2004;104:2285–310.
[28] Rurack K. Flipping the light switch 'ON' - the design of sensor molecules that show cation-induced fluorescence enhancement with heavy and transition metal ions. Spectrochim Acta Part A 2001;57:2161–95.
[29] Weng YQ, Yue F, Zhong YR, Ye BH. A copper(II) ion-selective on–off-type fluoroionophore based on zinc porphyrin–dipyridylamino. Inorg Chem 2007;46:7749–55.
[30] Murphy CB, Zhang Y, Troxler T, Ferry V. Probing förster and dexter energy-transfer mechanisms in fluorescent conjugated polymer chemosensors. J Phys Chem B 2004;108:1537–43.
[31] Zhang XB, Guo CC, Li ZZ. An optical fiber chemical sensor for mercury ions based on a porphyrin dimer. Anal Chem 2002;74:821–5.
[32] Chaparadza A, Rananavare SB. Room temperature Cl_2 sensing using thick nanoporous films of Sb-doped SnO_2. Nanotechnology 2008;19:245501–8.
[33] Lohani CR, Lee KH. The effect of absorbance of Fe^{3+} on the detection of Fe^{3+} by fluorescent chemical sensors. Sensor Actuators B Chem 2010;143:649–54.
[34] Hung CH, Chang GF, Kumar A. m-Benziporphodimethene: a new porphyrin analogue fluorescence zinc(II) sensor. Chem Commun 2008:978–80.
[35] Ozmen B, Akkaya EU. Infrared fluorescence sensing of submicromolar calcium: pushing the limits of photoinduced electron transfer. Tetrahedron Lett 2000;41:9185–8.
[36] Joshi BP, Park J, Lee WI, Lee KH. Ratiometric and turn-on monitoring for heavy and transition metal ions in aqueous solution with a fluorescent peptide sensor. Talanta 2009;78:903–11.
[37] Li L, Sun Y, Wang S, Qiu M. New fluorescent probes based on supramolecular diastereomers for the detection of 2-nitrophenol. Talanta 2010;81:1643–9.
[38] Crosby GA, Demas JN. Measurement of photoluminescence quantum yields. Rev J Phys Chem 1971;75:991–4.
[39] Chauvin AS, Frapart YM, Vaissermann J. Synthesis, X-ray crystal structure, and redox and electronic properties of iron(III)–polyimidazole complexes relevant to the metal sites of iron proteins. Inorg Chem 2003;42:1895–900.
[40] Ohta H, Sunatsuki Y, Kojima M. Supramolecular spin-crossover iron complexes based on imidazole–imidazolate hydrogen bonds. Inorg Chem 2004;43:4154–71.
[41] Laurent B, Halut S, Donnadieu B. Monomeric iron(II) hydroxo and iron(III) dihydroxo complexes stabilized by intermolecular hydrogen bonding. Inorg Chem 2006;45:2403–5.